Bioorganic Chemistry 53 (2014) 15–23

Contents lists available at ScienceDirect

Bioorganic Chemistry

journal homepage: www.elsevier.com/locate/bioorg

Synthesis, characterization and *in vitro* anti-neoplastic activity of gypsogenin derivatives

Safiye Emirdağ-Öztürk [a], İlknur Babahan [b,*], Ali Özmen [c]

[a] Chemistry Department, Faculty of Science, Ege University, Bornova, İzmir 35100, Turkey
[b] Chemistry Department, Adnan Menderes University, Aydin 09010, Turkey
[c] Biology Department, Adnan Menderes University, Aydin 09010, Turkey

ARTICLE INFO

Article history:
Received 21 August 2013
Available online 25 December 2013

Keywords:
Gypsogenin
vic-Dioxime
Thiosemicarbazone
Transition metal complex
Antiproliferative
Leukemia

ABSTRACT

Gypsogenin (**L^1**; *3-hydroxy-23-oxoolean-12-en-28-oic acid*), a natural saponin, was isolated from the boiling water extract of *Gypsophila arrostii* roots. In addition, the derivatives gypsogenin thiosemicarbazone (**L^2**; *23-[(aminocarbonothioyl)hydrazono]-3-hydroxolean-12-en-28-oic acid*) and gypsogenin thiosemicarbazone glyoxime (**L^{3}H$_2$**; *(3β)-3-hydroxy-23-[({[(1Z,2E)-N-hydroxy-2-(hydroxyimino)ethanimidoyl]amino}carbonothioyl)hydrazono] olean-12-en-28-oic acid*) as well as the Cu(II) and Co(II) complexes of **L^{3}H$_2$** were prepared. The structures were established on NMR analysis (^{1}H, ^{13}C NMR, HMBC, HMQC, and NOESY), FT-IR and completed by analysis of LC/MS. Furthermore, the antiproliferative effects of the Co(II) and Cu(II) complexes of the gypsogenin derivatives were assayed in human promyelocytic leukemia (HL 60) cells. These complexes were found to be potent anticancer agents with concentrations that inhibited 50% of proliferation (I_pC_{50}) between 5 μM and 40 μM. Cell death was distinguished by HO/PI double staining. The Co(II) complex of **L^{3}H$_2$** has shown approximately %50 apoptotic effect at 10 μM concentration. Paclitaxel has been used as positive control.

1. Introduction

The Gypsophila genus is well known to contain saponins, which have industrial interest due to their various applications. For example, saponins from the roots of *Gypsophila paniculata* and *Gypsophila arrostii* have been used as detergents and expectorants [1,2]. In addition, Gypsophila saponins have been found to posess various biological activities such as antimicrobial [3] and antioxidant [4] activities.

Gypsogenin, a natural saponin, is obtained from the roots of *G. arrostii* [5]. Gypsogenin from this plant can inhibit the growth and metastasis of Lewis lung cancer and triggers apoptosis by increasing Bax levels [6]. *Momordica charantia*, a famous medicinal plant used in various Asian traditional medicines also contains gypsogenin [7]. Gypsogenin from Momordica roots possesses anticancer activities against L1210, CCER-CEM and Ls174T cancer cells [6].

Thiosemicarbazones are potent antitumor agents that inhibit topoisomerase II. Recently, di-2-pyridylketonethiosemicarbazone and 2-benzoylpyridine thiosemicarbazone ligands have shown selective antitumor activity *in vitro* and also *in vivo* [8]. 3,5-Diacetyl-1,2,4-triazolbis(4,4-dimethylthiosemicarbazone) ligand, H(3)L(1), and its dinuclear platinum complex [Pt(muHL(1))](2) exhibit high antiproliferative activity in human non-small cell lung cancer NCI-H460 cells [9]. In addition, the antitumor activities of gallium(III) and iron(III) complexes with five different 4N-substituted R—N-heterocyclic thiosemicarbazones have been studied against two human cancer cell lines (41M and SK-BR-3) *in vitro*. It was found that gallium(III) enhances the cytotoxic activity [10]. Furthermore, six metal complexes of heterocyclic thiosemicarbazones have been tested against K562 leucocythemia cancer cells. All the tested compounds showed significant antitumor activity [11]. Moreover, the antitumor activities and mechanisms of 1,2-naphthoquinone-2-thiosemicarbazone and its metal complexes (Cu^{2+}, Pd^{2+} and Ni^{2+}) have been investigated against human MCF-7 breast cancer cells. The results revealed that these complexes are effective at inhibiting MCF-7 cell growth [12]. Additionally, heterocyclic thiosemicarbazones, thioureas and 2-substituted pyridine N-oxides as well as representative nickel, cobalt and copper complexes have been shown to be potent antineoplastic/cytotoxic agents. The cytotoxic activity of these agents was demonstrated against single cell leukemia as well as cell lines derived from solid tissues (colon adenocarcinoma, HeLa, KB, skin, bronchogenic lung, bone osteosarcoma and glioma). Furthermore, in L1210 cells, DNA synthesis and subsequently RNA synthesis have been shown to be inhibited by these agents [13].

Thus, the importance of coordination compounds as therapeutic agents has been increasingly demonstrated in a variety of systems.

* Corresponding author. Fax: +90 256 213 5379.
E-mail address: ilknurbabahan@yahoo.com (İ. Babahan).

0045-2068/$ - see front matter © 2013 Elsevier Inc. All rights reserved.
http://dx.doi.org/10.1016/j.bioorg.2013.12.001

In particular, "*vic*-dioxime compounds" have been investigated owing to their resemblance to vitamin B_{12} and chlorophyll [7].

Here, as part of our ongoing studies, we report the isolation of the known saponin gypsogenin ($\mathbf{L^1}$) and the synthesis and potential anticancer activity of new gypsogenin ligands (gypsogenin thiosemicarbazone ($\mathbf{L^2}$) and gypsogenin thiosemicarbazone glyoxime ($\mathbf{L^3H_2}$). In addition, we determined the antiproliferative activities of the novel Cu(II) and Co(II) complexes of $\mathbf{L^3H_2}$ for the first time using human promyelocytic leukemia (HL 60) cells. The Cu(II) complex of $\mathbf{L^3H_2}$ was determined to have the strongest antiproliferative activity, with an I_pC_{50} value of 5 μM. Also the Co(II) complex has shown strong antiproliferative effect at 5 μM concentration.

2. Results and discussion

The starting material gypsogenin ($\mathbf{L^1}$) was isolated from the boiling water extract of *G. arrostii* roots (Scheme 1, Fig. 1). The novel gypsogenin thiosemicarbazone ($\mathbf{L^2}$) was prepared by condensation of gypsogenin with thiosemicarbazide in MeOH. The other novel ligand, *vic*-dioxime bearing gypsogenin and thiosemicarbazone groups ($\mathbf{L^3H_2}$), was synthesized by reacting *(E,E)*-dichloroglyoxime with gypsogenin thiosemicarbazone ($\mathbf{L^2}$) (Scheme 2, Fig. 2). The trinuclear Cu(II) and Co(II) complexes were prepared from the $\mathbf{L^3H_2}$ derivative with a stoichiometric amount of $CoCl_2{\cdot}6H_2O$ and $CuCl_2{\cdot}2H_2O$, respectively, in ethanol (Scheme 4).

The new ligands were characterized by ^1H NMR, ^{13}C NMR, HMBC, HMQC, NOESY, FT-IR and LC/MS. Attempts to isolate crystals suitable for X-ray diffraction were unsuccessful for both the ligands and complexes. In addition, FT-IR, MS and magnetic susceptibility techniques were employed to determine the structural characteristics of the metal complexes. Finally, the antiproliferative effects of the Cu(II) and Co(II) complexes were determined using HL 60 cells.

2.1. IR Spectra

The FT-IR data of the ligands and their complexes are provided in Table 1. The IR spectra of compounds $\mathbf{L^1}$, $\mathbf{L^2}$ and $\mathbf{L^3H_2}$ exhibited —NH (3435 cm^{-1} for $\mathbf{L^2}$ and 3464 cm^{-1} for $\mathbf{L^3H_2}$), —OH (3463 cm^{-1} for $\mathbf{L^1}$, 3300 cm^{-1} for $\mathbf{L^2}$ and 3310 cm^{-1} for $\mathbf{L^3H_2}$), —C=N_{oxime} (1550 cm^{-1} for $\mathbf{L^3H_2}$), —C=$N_{thiosemicarbazone}$ (1600 cm^{-1} for $\mathbf{L^2}$ and 1681 cm^{-1} for $\mathbf{L^3H_2}$), and —NO (1020 for $\mathbf{L^3H_2}$) stretching vibrations [14,15].

The C=N and OH stretching vibrations are similar to other reported *vic*-dioxime derivatives [14]. The IR spectrum of $\mathbf{L^2}$ showed a stretching band of C=S at 821 cm^{-1} and an absorption band of the —NH_2 group at 3717 cm^{-1}.

Coordination of sulfur with the metal ion would result in the displacement of electrons towards the latter, thus resulting in weakening of the C=S bond. Hence, on complexation, C=S stretching vibrations should decrease [16]. Therefore, on complexation, the frequency of the peak at 849 cm^{-1} was shifted to a lower wave number and the intensity of the peak was also reduced. All these changes on complexation confidently showed the presence of a metal–sulfur bond.

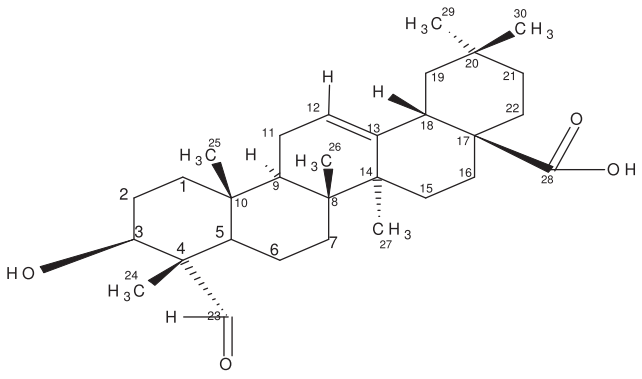

Scheme 1a. Structure of Gypsogenin ($\mathbf{L^1}$).

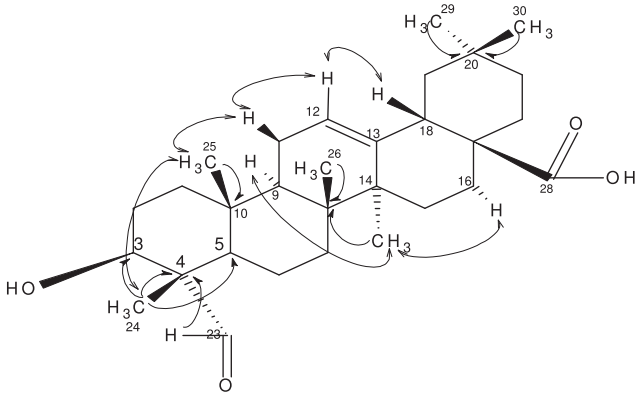

Scheme 1b. Selected HMBC (single-headed arrows) and NOESY (double-headed arrows) correlations of Gypsogenin ($\mathbf{L^1}$).

Fig. 1. Picture of *Gypsophila arrostii*.

The possibility of thione–thiol tautomerism (Scheme 3, H—N—C=S, C=N–SH) in these ligands was ruled out by the absence of characteristic thiol bands near 2700–2500 cm^{-1} in the IR spectrum [16]. The observation of strong ν(C=S) absorption bands near 849–821 cm^{-1} in the IR spectra of the ligands also suggested that they are in the thione tautomeric form in the solid state.

The far IR spectral bands in both the ligands were practically unchanged in the complexes, but they showed some new bands with medium to weak intensity in the 693–519 cm^{-1} region, tentatively assigned to ν(M—N) and ν(M—S), which are in agreement with previous works [17].

The FT-IR spectra of KBr pellets containing the gypsogenin thiosemicarbazone glyoxime complexes of the general formula $M_3(LH)_2$, in which M is Cu(II) or Co(II).$2H_2O$, exhibited C=N_{oxime}, C=$N_{thiosemicar.}$ and C=S absorptions at 1532–1528 cm^{-1}, 1631–1630 cm^{-1} and 832–830 cm^{-1}, respectively. These bands suggest that the ligands are N,N′ and N,S coordinated with the metal ion according to the proposed structures depicted in Scheme 4.

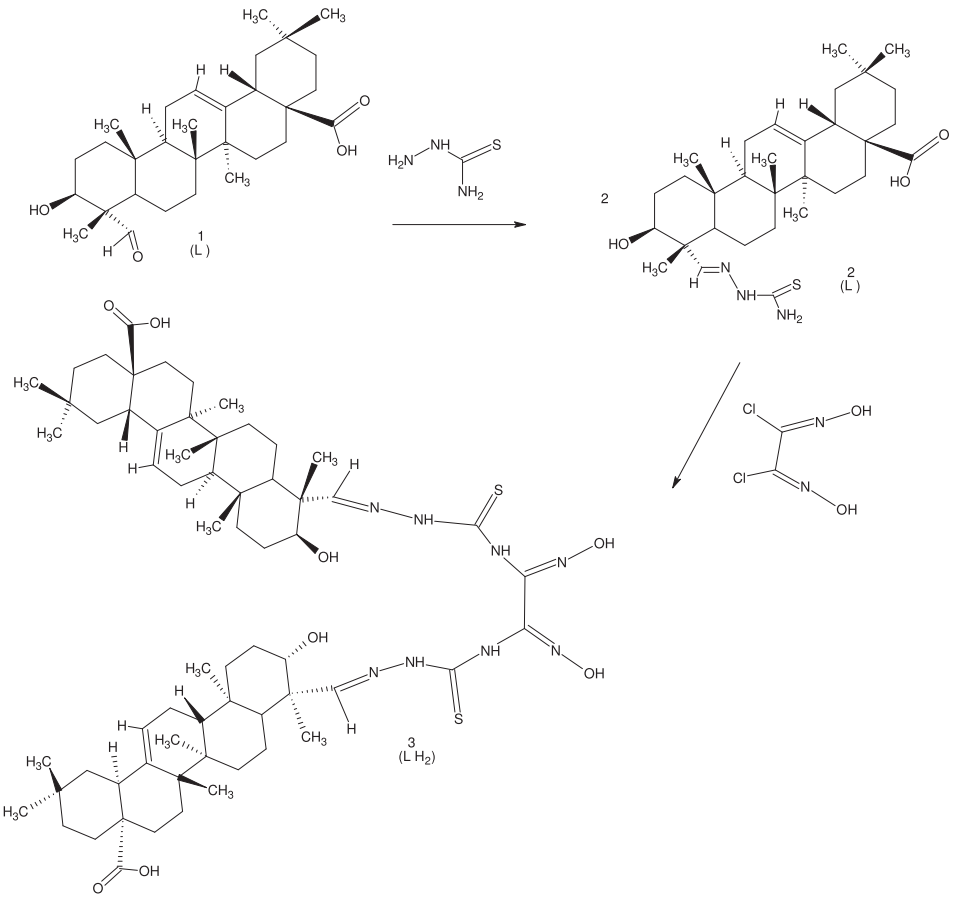

Scheme 2. Synthesis of $\mathbf{L^2}$ and $\mathbf{L^3H_2}$.

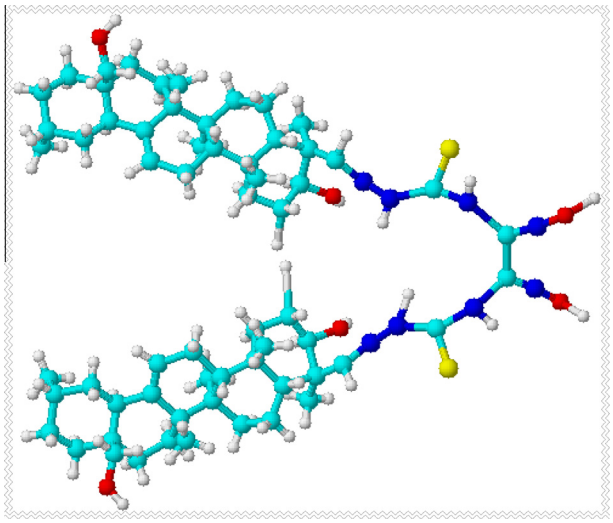

Fig. 2. Proposed structure of $\mathbf{L^3H_2}$.

The dioxime ligand is a neutral compound; in the complexes, it is a monoanion formed by the loss of an oxime proton with the concomitant formation of an intramolecular hydrogen bond. It is known that Co(II) and Cu(II) metal complexes of dimethylglyoxime are 5-membered chelate structures and the metal ion coordinates to the nitrogen atoms of the dioxime groups. A hydrogen atom separates each of the 2 oxime groups, and as a result a hydrogen bridge is established [18a–d]. The hydrogen bridge (O—H···O) bonds of the $\mathbf{[Cu_3(L^3H)_2]}$ and $\mathbf{[Co_3(L^3H)_2(H_2O)_6]}$ complexes appear at 1775 and 1869 cm^{-1}, respectively.

2.2. ^1H and ^{13}C NMR spectra of the ligands

^1H NMR and ^{13}C NMR data of the ligands are listed in Tables 2 and 3. The ^1H NMR spectrum of gypsogenin ($\mathbf{L^1}$) indicated six methyl signals (δ_H 2.48, 2.01, 2.11, 2.40, 2.08 and 2.13), one aldehyde proton signal (δ_H 10.75). In the ^{13}C NMR spectrum, a total of 30 carbons was observed. These assignments of the ^1H and ^{13}C NMR resonance based on NOESY, HMQC and HMBC NMR spectra. Gypsogenin ($\mathbf{L^1}$) showed two carbonyl peaks (δ_C 206.87, aldehyde, and δ_C 179.85, carboxylic). The proton and carbon chemical shifts were assigned by HMQC. The ^{13}C NMR spectrum of gypsogenin ($\mathbf{L^1}$) showed olefinic carbon signals at δ_C 122.02 (C-12) and 144.64 (C-13). The H-3, H-12, H-18 proton signals were strongly supported by HMQC spectrum at δ_H 5.20, 6.62, and 4.43, respectively. The C-23 aldehydic proton (δ_H 10.75) showed HMBC interactions (Scheme 1b) with carbon signals at 56.04 (C-4). Other significant HMBC correlations were observed the H-24 (δ_H 2.48) and four carbon signals at δ_C 71.38 (C-3), 56.04 (C-4), 47.46 (C-5), and 206.87 (C-23). The signals in the ^{13}C NMR spectrum were those for six methyl carbons (δ_C 9.51, 15.34, 17.35, 25.93, 33.97 and 23.54), one hydroxy carbon at δ_C 71.38 (C-3). The NOESY spectrum showed correlation between H-25 and the axial methyl group H-24. Thus, the aldehyde group at C-4 was observed as equatorial coupling constant. Also, the equatorial position of H-12 was supported by the resonance position of H-18 (δ_H 4.43) and H-25 (δ_H 2.01). Selected HMBC and NOESY correlations used for assignment of the gypsogenin structure are presented in Scheme 1b (The

Table 1
Characteristic IR bands of the ligands and their metal complexes (cm^{-1}, KBr) (1) $\mathbf{L^1}$ (2) $\mathbf{L^2}$ (3) $\mathbf{L^3H_2}$ (4) $[Cu_3(L^3H)_2]$ (5) $[Co_3(L^3H)_2(H_2O)_6]$.

	NH_2/NH	—OH/H_2O	C=O	C=S	O—H···O	C=N[a]	C=N[b]	N—O	M—N	M—S
1	–	3463 b	1717 s	–	–	–	–	–	–	–
2	3717 m 3435 b	3300 b	1702 s	821 m	–	1600 s	–	–	–	–
3	3464 b	3310 b	1726 s	849 m	–	1681s	1550 s	1020 m	–	–
4	3445 b	3320 b	1725 s	832 m	1775 w	1631s	1532 s	1014 m	580 m	519 m
5	3495 b	3340 b	1723 s	830 m	1869 w	1630 s	1528 s	1010 m	693 m	520 m

b: Board s: strong, m: medium, w: weak.
[a] ν(C=N): thiosemicarbazone moiety.
[b] ν(C=N): oxime moiety.

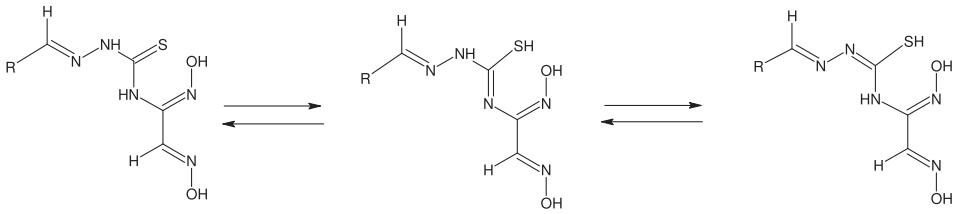

Scheme 3. Thione (I) and thiol (II and III) forms of $\mathbf{L^3H_2}$ (R: Gypsogenin for $\mathbf{L^3H_2}$).

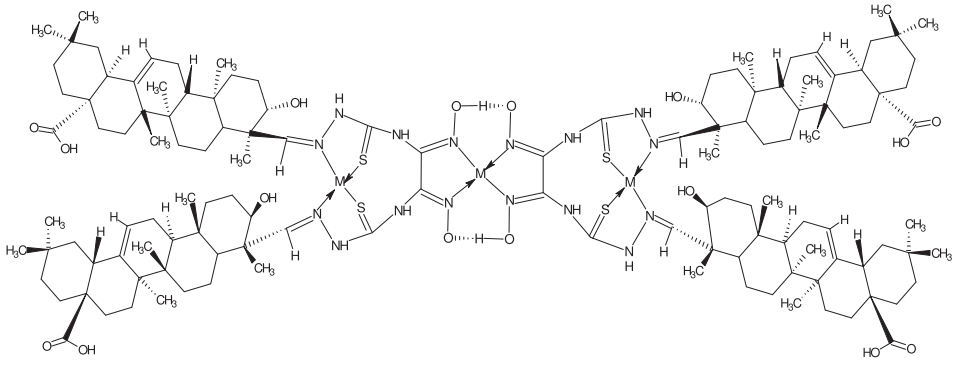

Scheme 4. Suggested structure of the Cu(II) and Co(II)·$2H_2O$ complexes for $\mathbf{L^3H_2}$.

spectra of HMBC, HMQC and NOESY were given in Figs. S1–S5 for L^1 in Supplementary materials). Table 2 summarizes all observed correlations.

The ^{1}H NMR spectrum of $\mathbf{L^2}$ showed the signal of H-23 at δ_H 7.94 instead of δ_H 10.75 in $\mathbf{L^1}$ (gypsogenin). The —C=SN**H** signal was displayed at δ_H 9.01. In the ^{13}C NMR spectrum, the signals belonging to —N=**C**H and NH_2**C**=S appeared at δ_C 157.01 and 180.45, respectively. The CH_3 signals were shown at 12.15, 14.59, 17.71, 26.47, 34.35 and 23.25 ppm for $\mathbf{L^2}$ (Table 3).

In the ^{1}H NMR spectrum of $\mathbf{L^3H_2}$, the absence of —NH_2 functional groups (δ = 9.58 ppm for $\mathbf{L^2}$) and the presence of new —NH and —OH groups at δ = 9.21 and 10.93 ppm indicate the formation of new compound which contains vic-dioxime and thiosemicarbazone macrocyclic moiety. The observation of these singlets provides confirmation of gypsogenin thiosemicarbazone ($\mathbf{L^2}$) reaction with anti-dichloroglyoxime.

When the ^{1}H NMR spectrum of the ligand $\mathbf{L^3H_2}$ in DMSO was examined, peaks corresponding N—OH protons were observed at 10.93 ppm (s, 2H) [19–22]. The peaks of NH protons appeared at 7.92 ppm (s, 2H, CNN**H**) and 9.21 ppm (s, 2H, CSN**H**) for $\mathbf{L^3H_2}$ [16–23]. In agreement with the IR data, other evidence of the thione form of the ligands was the appearance of NH signals around 9.21–7.92 ppm in the ^{1}H NMR spectrum.

The disappearance of these peaks by the addition of D_2O to the ligand solution indicated that the observed resonances are those of the protons of O—H and N—H groups. These values are in accord with previously reported oxime derivatives [19–24]. In addition, the peaks of the —C**H**=N-NH protons of azomethine appeared at 7.33 ppm (s, 2H) for $\mathbf{L^3H_2}$ (Table 3). The CH_3 peaks of $\mathbf{L^3H_2}$ were observed in agreement with the literature data, at δ = 1.10, 1.04, 0.85, 0.82, 0.71, 0.69 ppm, respectively (Table 3).

In the ^{13}C NMR spectrum of the $\mathbf{L^3H_2}$ ligand, one signal was observed at 161.28 ppm, corresponding to HN**C**=N—OH, which shows symmetrically substituted *vic*-dioxime [19–26].

The peak corresponding to H**C**=N—N appeared at 157.77 ppm for $\mathbf{L^3H_2}$ [29–31]. Moreover, C=S and C=O peaks of $\mathbf{L^3H_2}$ were observed at 174.53 and 175.32 ppm respectively. The CH_3 signals appeared at 33.98, 26.31, 22.39, 17.99, 12.07 and 11.63 ppm for $\mathbf{L^3H_2}$ [27–31].

2.3. MS analysis

The LSMS/APCI of gypsogenin ($\mathbf{L^1}$) showed a molecular ion peak at *m/z* 470.2 $[M+H]^+$, consistent with a molecular formula of $C_{30}H_{40}O_4$. Likewise, the molecular formula of $\mathbf{L^2}$ was established as $C_{31}H_{49}O_3N_3S$ by LSMS/APCI mass spectroscopy (543.3 $[M+H]^+$, 452.0 $[M-(H_2N-CS-NH-N)-H]^+$ and 453.0 $[M-(H_2N-CS-NH-N)]^+$). Similarly, FAB mass spectral analysis indicated molecular ion *m/z* ratios of 1171 $[M]^+$ for $\mathbf{L^3H_2}$, in agreement with

Table 2
^{1}H and ^{13}C NMR spectra of the ligand for $\mathbf{L^1}$ (400 MHz δ ppm, in pyridine).

Position	$\delta^{13}C$	$\delta^{1}H$[a]	HMBC[b] (H to C)	NOESY
1	38.24, CH_2	2.66 (m), 2.17 (m)		
2	28.02, CH_2	3.23 (m), 2.26 (m)		24
3	71.38, CH	5.20		
4	56.04, qC	–		
5	47.46, CH	2.58 (m)		25
6	20.97, CH_2	2.61 (m), 2.29 (m)		
7	32.78, CH_2	2.59 (m), 2.31 (m)	6	
8	39.81, qC	–		
9	47.84, CH	2.89 (m)		27
10	35.81, qC	–		
11	26.82, CH_2	2.98 (m), 2.46 (m)		12, 25
12	122.02, CH	6.62 (br s)		11, 18, 25
13	144.64, qC	–		
14	42.21, qC	–		
15	30.85, CH_2	2.61 (m)		
16	23.82, CH_2	3.25 (m), 3.06 (m)		27
17	46.62, qC	–		
18	41.76, CH	4.43 (dd, J = 13.6 Hz, J = 4.0 Hz)		12
19	46.22, CH_2	2.92 (m), 2.45 (m)		27, 29
20	32.32, qC	–		
21	35.50, CH_2	2.56 (m), 2.35 (m)		29, 30
22	33.05, CH_2	3.15 (m), 2.93 (m)		
23	206.87, CH	10.75 (s)	4	
24	9.51, CH_3	2.48 (s)	3, 4, 5, 23	2, 25
25	15.34, CH_3	2.01 (s)	10	5, 11, 12, 24
26	17.35, CH_3	2.11 (s)	8, 9	
27	25.93, CH_3	2.40 (s)	8, 13, 14	9, 16, 19
28	179.85, qC	–		
29	33.97, CH_3	2.08 (s)	20, 30	19, 21
30	23.54, CH_3	2.13 (s)	20	21

[a] Multiplicity of signals is given in parentheses: s, singlet; d, doublet; m, multiplet; and br, broad.
[b] Identified from the HMQC spectrum.

the proposed structure (Fig. S6 for L3H2 in Supplementary materials).

Furthermore, FAB mass spectral analysis indicated m/z ratios of 2531 $[M]^+$ for the Cu(II) complex and 2625 $[M-1]^+$ for the Co(II) complex. Thus, the ligand ($\mathbf{L^3H_2}$) was determined to form mononuclear complexes [$(\mathbf{L^3H})_2\underline{\mathbf{M_3}}$] with a metal to ligand ratio of 3:2 with M = $Co(II)(H_2O)_2$ and Cu(II).

2.4. Magnetic susceptibility

The room temperature magnetic moment measurements showed that the Co(II) complex is paramagnetic with a magnetic susceptibility of 3.72 B.M. for $\mathbf{L^3H_2}$ per Co(II). The magnetic susceptibility values of Co(II) complexes are within the range of high spin octahedral Co(II) complexes (the three-spin value is 3.87 B.M.) [32]. Thus, the Co(II) complex of the ligand was determined to be octahedral with water molecules as axial ligands.

The Cu(II) complex also was found to be paramagnetic with μ_{eff} = 1.70 for $\mathbf{L^3H_2}$ per Cu(II) ion. These values fit the spin value of 1.73 B.M. Though these are somewhat low values for the magnetic moments, some diamagnetism is likely contributed from the ligand, which ultimately decreases the total paramagnetism of the complex [19]. Thus, the Cu(II) complex was found to have a square planar geometry.

2.5. Antiproliferative activity

The antiproliferative activities of the three ligands, gypsogenin ($\mathbf{L^1}$), gypsogenin thiosemicarbazone ($\mathbf{L^2}$) and gypsogenin thiosemicarbazone glioxime ($\mathbf{L^3H_2}$), and their Cu(II) and Co(II) complexes were analyzed using cultured HL-60 cells. The HL-60 cell line is a leukemic cell line that is commonly used for laboratory research because it provides a continuous source of human cells for studying the molecular events of myeloid differentiation and the effects of physiological, pharmacological and virologic elements on this process.

Among the tested compounds, gypsogenin, $\mathbf{[Cu_3(L^3H)_2]}$ and $\mathbf{[Co_3(L^3H)_2(H_2O)_6]}$ were found to be potent anticancer agents due to their strong antiproliferative effects, with a concentration that inhibited 50% of proliferation (I_pC_{50}) between 5 μM and 10 μM (Figs. 3–5). The strongest antiproliferative activity was determined with the $[Cu_3(L^3H)_2]$ complex (Fig. 4a). Paclitaxel has been used in this study as positive control. Paclitaxel is a mitotic inhibitor used in cancer chemotherapy. It prevents microtubule depolymerization and blocks normal cell division. Paclitaxel has inhibited min. %50 of cells at 1 μM concentration.

Gypsogenin and the $\mathbf{[Co_3(L^3H)_2(H_2O)_6]}$ complex also showed similarly strong antiproliferative activities as $\mathbf{[Cu_3(L^3H)_2]}$ (Figs. 3 and 4). However, the other ligands ($\mathbf{L^2}$ and $\mathbf{L^3H_2}$) of these derivatives showed weak antiproliferative activities (data not shown) against HL-60 cells.

In comparison with positive control the tested complexes showed nearly the same effect but in concentrations between 1 μM and 5 μM. If considered as a drug this range is not high for an active substance.

In addition, the apoptotic effects of gypsogenin, $\mathbf{[Cu_3(L^3H)_2]}$ and $\mathbf{[Co_3(L^3H)_2(H_2O)_6]}$ were determined by the Hoechst 33258/propidium iodide double staining method. Only the very late phenotypes of apoptosis can be visualized by phase contrast microscopy, but the quantification of cell death is impossible. So the combination of microscopic examination together with a double staining method with fluorescent dyes is a very reliable and sensitive method to determine the type of cell death and quantify it. Hoechst 33258 (HO) and Propidium iodide (PI) both stain chromatin. When HOPI-stained cells are examined under the microscope also early stages of death are detected and can

Table 3
^{1}H and ^{13}C NMR spectra of the ligand for $\mathbf{L^2}$ (400 MHz δ ppm, in pyridine) and for $\mathbf{L^3H_2}$ (400 MHz δ ppm, in DMSO-d6).

Position	$\mathbf{L^2}$		$\mathbf{L^3H_2}$	
	$\delta^{13}C$	$\delta^{13}H$[a]	$\delta^{13}C$	$\delta^{1}H$[a]
1	38.89, CH_2	1.92 (m), 1.37 (m)	39.46, CH_2	1.48 (m), 0.86 (m)
2	28.60, CH_2	2.36 (m), 1.46 (m)	28.48, CH_2	1.78 (m), 0.88 (m)
3	75.22, CH	4.19	75.72, CH	4.12
4	52.24, qC	–	52.50, qC	–
5	48.58, CH	1.79 (m)	47.57, CH	1.19 (m)
6	20.69, CH_2	1.89 (m), 1.49 (m)	20.16, CH_2	1.28 (m), 0.90 (m)
7	32.45, CH_2	1.86 (m), 1.5 1 (m)	33.53, CH_2	1.22 (m), 0.96 (m)
8	40.36, qC	–	42.16, qC	–
9	48.67, CH	2.01 (m)	48.11, CH	1.51 (m)
10	37.09, qC	–	36.79, qC	–
11	27.52, CH_2	2.19 (m), 1.61 (m)	26.59, CH_2	1.65 (m), 1.08 (m)
12	122.68, CH	5.78 (br s)	120.40, CH	5.02 (br, s)
13	145.16, qC	–	142.40, qC	–
14	42.51, qC	–	42.37, qC	–
15	30.29, CH_2	1.90 (m)	30.05, CH_2	1.31 (m)
16	24.10, CH_2	2.42 (m), 2.26 (m)	24.38, CH_2	2.48 (m), 1.69 (m)
17	46.97, qC	–	47.27, qC	–
18	42.34, CH	3.59 (d, J = 10.0 Hz)	41.92, CH	2.86 (d, J = 10.2 Hz)
19	46.79, CH_2	2.11 (m), 1.58 (m)	46.24, CH_2	1.56 (m), 1.06 (m)
20	31.28, qC	–	31.35, qC	–
21	34.57, CH_2	1.73 (m), 1.53 (m)	34.76, CH_2	1.11 (m), 0.98 (m)
22	33.61, CH_2	2.33 (m), 2.14 (m)	34.90, CH_2	1.76 (m), 1.61 (m)
23	157.01, CH	7.94 (s)	157.77, CH	7.33 (s)
24	12.15, CH_3	1.65 (s)	11.63, CH_3	1.10 (s)
25	14.59, CH_3	1.22 (s)	12.07, CH_3	0.69 (s)
26	17.71, CH_3	1.29 (s)	17.99, CH_3	0.82 (s)
27	26.47, CH_3	1.55 (s)	26.31, CH_3	1.04 (s)
28	180.55, qC	–	175.32, qC	–
29	34.35, CH_3	1.26 (s)	33.98, CH_3	0.71 (s)
30	23.25, CH_3	1.31 (s)	22.39, CH_3	0.85 (s)
–**C**=S	180.45	–	174.53	–
–CNN**H**	–	9.01 (s)	–	7.92 (s)
–CSN$\mathbf{H_2}$	–	9.58 (s)	–	–
–CSN**H**	–	–	–	9.21 (s)
–**C**=NOH	–	–	161.28	10.93 (s)

[a] Multiplicity of signals is given in parentheses: s, singlet; d, doublet; m, multiplet; and br, broad.

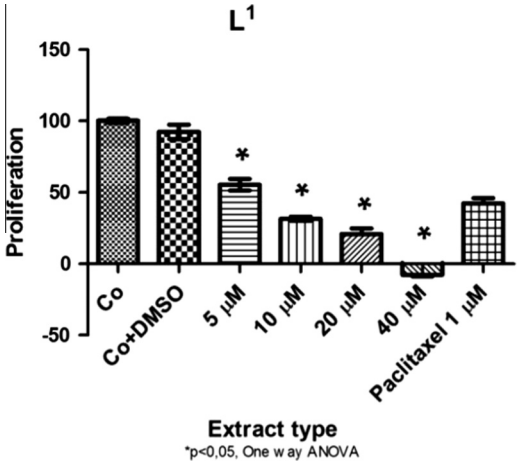

Fig. 3. Antiproliferative effect of $\mathbf{L^1}$.

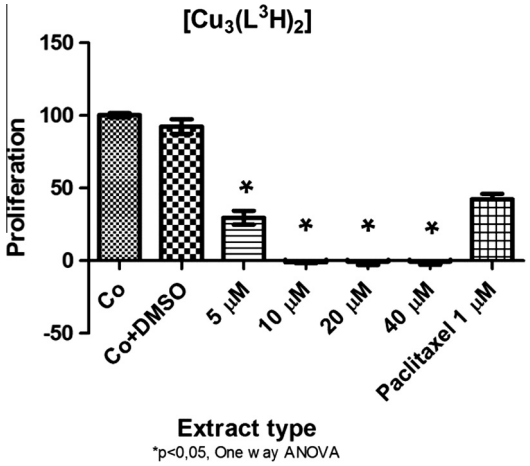

Fig. 4a. Antiproliferative effect of Cu(II) complex.

be quantified. In combination with the examination of condensed chromatin this method allows to discriminate between early or late apoptosis, necrosis and intact cells, because administration of both dyes either stains nuclei in blue when cells are viable or in a early to mid-apoptotic stage, or pink (interference of blue and red) when cells are in a late apoptotic stage or when necrotic (Fig. 6). The best apoptotic rate was determined with the $\mathbf{[Co_3(L^3H)_2(H_2O)_6]}$ complex (Fig. 5). Nearly 50% of the cells died through an apoptotic pathway. Paclitaxel used as positive control. Paclitaxel is a cytoskeletal drug that targets tubulin. Paclitaxel stabilizes the microtubule polymer. By this way it blocks progression of mitosis. As result of this apoptosis is triggered at the mitotic checkpoint. Paclitaxel showed about %50 apoptosis at 1 μM application. In this study only the $\mathbf{[Co_3(L^3H)_2(H_2O)_6]}$ complex can approached to this endpoint at 10 μM concentration. These findings support the antitumoral effects of gypsogenin and its derivatives that have been found by others for gypsogenin [33].

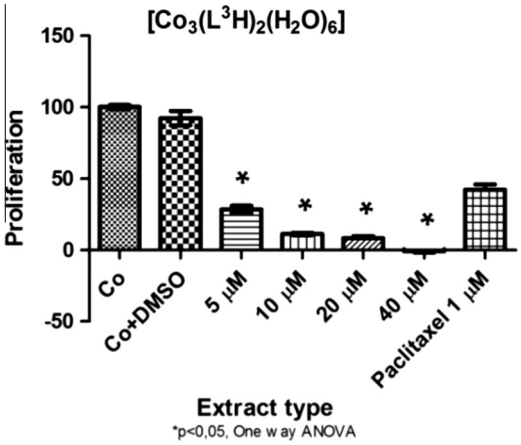

Fig. 4b. Antiproliferative effect of Co(II) complex.

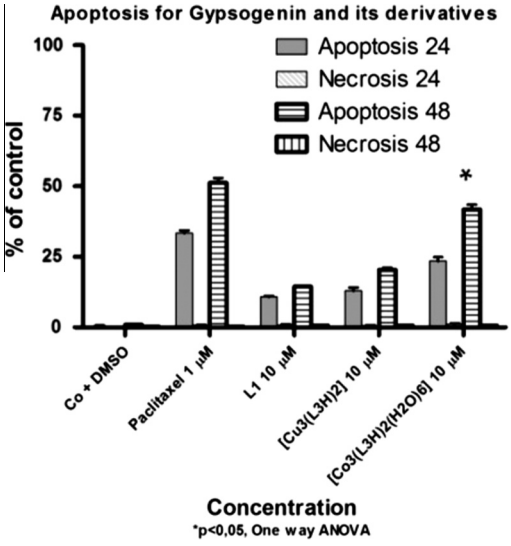

Fig. 5. Apoptosis for $\mathbf{L^1}$ and its derivatives.

Gypsogenin is a natural saponin and L^3H_2 was obtained from gypsogenin thiosemicarbazone ($\mathbf{L^2}$). Saponins are potential anticancer agents, with different mechanisms of action. Their cytotoxic effects may be due to either apoptosis inducement or non-apoptotic cell death stimulation. There is a number of well-known processes which lead to the same effect – cell death – but involve different mechanisms of action, like stimulation of autophagic cell death, decrease in NO production in cells, or cytoskeleton integrity disassembly [34].

Due to the surfactant properties of saponins they can be used to enhance penetration of macromolecules, e.g. proteins through cell membranes, making them useful as adjuvants in vaccines [35].

Moreover, thiosemicarbazone and oxime derivatives and their metal complexes also possess antiproliferative properties against tumor cells. The search for antitumoral drugs led to the discovery of several thiosemicarbazone derivatives having antitumoral activities. In agreement with these previous studies, our results support the antitumor activity of these agents.

Because of the unfavourable effects of cancer on the population, the search for new anticancer drugs is important to avoid the high costs of therapy and to improve the quality of life of patients. Cancer is the second leading cause of mortality in the USA. In 2007, 1.44 million people were afflicted with cancer and 559,650 died of cancer [36]. In 2002, 1.28 million individuals incurred cancer and the mortality rate was 38%. Thus, it is evident that there were not any changes in the mortality rates of cancer between 2002 and 2007 [37].

The aim for new anticancer drugs is to discover new structures that possess a specific mechanism of action. In this frame, gypsogenin ($\mathbf{L^1}$), gypsogenin thiosemicarbazone ($\mathbf{L^2}$) and gypsogenin thiosemicarbazone glioxime ($\mathbf{L^3H_2}$), and their Cu(II) and Co(II) complexes synthesized in this work can be considered as potential anticancer agents for further investigations.

3. Conclusions

In this study, we successfully synthesized, characterized and determined the cytotoxic activities of novel thiosemicarbazone and oxime gypsogenin derivatives for the first time. Gypsogenin ($\mathbf{L^1}$) as well as the Co(II) and Cu(II) complexes of gypsogenin thiosemicarbazone glyoxime ($\mathbf{L^3H_2}$) were found to be potent anticancer agents due to their antiproliferative effects on HL 60 cells. The Cu(II) complex of $\mathbf{L^3H_2}$ was determined to have the strongest antiproliferative activity, with an I_pC_{50} value of 5 μM.

4. Experimental

4.1. Chemistry

4.1.1. Materials and Instrumentation

All reagents used were purchased from Merck or Fluka. ^{1}H NMR, ^{13}C NMR, HMBC, HMQC, and NOESY spectra (Bruker 400 MHz), IR spectra (Varian 900), melting points (Buchi SPM-20) and pH measurements (Orion Expandable Ion Analyzer EA 940) were used to

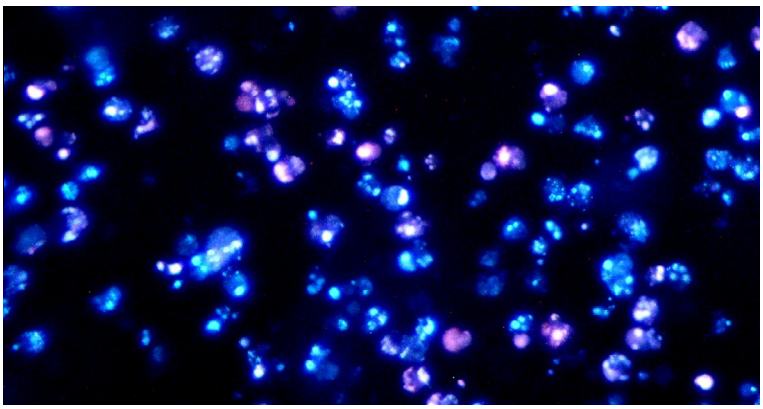

Fig. 6. Early and late apoptotic cells observed by HO/PI double staining (48 h). Photographed by Ali ÖZMEN-2013.

elucidate the structures of the products. MS spectra were recorded on an LC/MS Thermo MSQ Plus. The magnetic moments of the complexes were measured by the Gouy method with a Newport type D-104 instrument magnet power supply.

4.1.2. General method for the preparation of gypsogenin (L^1)

Gypsogenin was isolated from Gypsophila arrostii (Fig. 1). Water-extract of the roots of Gypsophila arrostii (400 mL) with ethanol (100 mL) was hydrolyzed with 10% KOH at 100 °C for 2 days. The reaction mixture was collected and neutralized with HCl. Then, this mixture was hydrolyzed with 10% HCl for 3 days. After hydrolyzed, this reaction mixture was neutralized with KOH and extracted with CH_2Cl_2. The CH_2Cl_2 phase is 1.4504 g. The mixture was purified by CC using silica gel and hexane/ethyl acetate (6/4) to afford gysogenin (325 mg); m.p. 273 °C (Schemes 1a and b).

4.1.3. Synthesis of Gypsogenin thiosemicarbazone (L^2)

A solution of thiosemicarbazide (1.5 mol) in water (7 mL) was added to a solution of gypsogenin (1.0 mol) in MeOH (7 mL). The mixture was refluxed for 13 h and then stirred at room temperature for 48 h. The reaction mixture was extracted with CH_2Cl_2 (3×10 mL). The organic layer was dried over anhydrous sodium sulfate and evaporated to dryness. The residue was chromatographed on silica gel using hexane/ethyl acetate (6:4) to give $\mathbf{L^2}$ (73 mg); m.p. 243 °C.

4.1.4. Synthesis of Gypsogenin thiosemicarbazone glyoxime (L^3H_2)

A solution of Gypsogenin thiosemicarbazone ($\mathbf{L^2}$) (1 mmol) in absolute ethanol 30 mL was added dropwise to a solution of antidichloroglyoxime (Scheme 2) (1 mmol) in absolute ethanol 10 mL for a 30 min period. The reaction mixture was stirred overnight at room temperature. After cooling to 0 °C the pH of the mixture was raised to 5.0–5.5 with treatment with $NaHCO_3$ dissolved in 5 mL distilled water, and stirring was continued for 1 h. The solution was poured into 100 mL cold water with stirring. After the end of the period, yellow precipitated solid was filtered, washed thoroughly with distilled water and dried. The chemical reaction and molecular structure are shown in Scheme 2. Results of the compositional and spectroscopic analyses are as follows: Yield; (60%) m.p. 283 °C Dec.

4.1.5. Synthesis of the Cu(II) and Co(II) Complexes of L^3H_2

A solution of a metal salt (3 mmol, 0.510 g of $CuCl_2{\cdot}2H_2O$ or 3 mmol 0.711 g $CoCl_2{\cdot}6H_2O$ in 50 mL of water) was added to 2 mmol of the ligand solution (2.34 g for $\mathbf{L^3H_2}$ in 50 mL of ethanol) with stirring. An initial sharp decrease in the pH of the solution from 5.5 to about 3–3.5 was observed. After raising the pH to 5–5.5 using a 1% aqueous NaOH solution, the reaction mixture was kept in a hot water bath (60 °C) for 2 h to complete the precipitation. Then the precipitated complexes were filtered, washed with water and dried at room temperature in a vacuum oven. Results of the compositional and spectroscopic analyses are shown as follows. Proposed structures of complexes are shown in Scheme 4.

$[Cu_3(L^3H)_2]$; Color: Brown, Yield; (43%), m.p.; >300 °C.
$[Co_3(L^3H)_2(H_2O)_6]$; Color; Brown, Yield; (65%), m.p.; >300.

4.2. Pharmacology

4.2.1. Cell culture

HL-60 promyeloic leukemia cells were purchased from ATCC. Cells were grown in RPMI-1640 medium supplemented with 10% heat inactivated fetal calf serum, 1% L-glutamine and 1% penicillin/streptomycin at 37 °C in a humidified atmosphere containing 5% CO_2.

4.2.2. Proliferation inhibition analysis

HL 60 cells were seeded in T-25 tissue culture flasks at a concentration of 1×10^5/mL and incubated with increasing concentrations of agents (corresponding to 5, 10, 20 and 40 μM of the drug). Cell counts and IC_{50} values were determined at 24 and 72 h using a Thoma slide. Experiments were done in triplicate. The percent of cell divisions compared to the untreated control were calculated as follows: [(C72 h + drug − C24 h + drug)/(C72 h − drug − C24 h − drug)] × 100 = % cell division, where C72 h + drug is the cell number after 72 h of drug treatment, C24 h + drug, is the cell number after 24 h of drug treatment, C72 h − drug is the cell number after 72 h without drug treatment, and C24 h − drug, is the cell number after 24 h without drug treatment.

4.2.3. Hoechst 33258 and propidium iodide double staining

HL-60 cells (1×10^5/mL) were seeded in T-25 Nunc tissue culture flask and exposed to these complexes and drug for 24 and 48 h. Cell death quantification by Hoechst 33258 and propidium iodide staining, which facilitates to distinguish between apoptosis and necrosis, was performed according to the method described by Grusch et al. [38].

Appendix A. Supplementary material

Supplementary data associated with this article can be found, in the online version, at http://dx.doi.org/10.1016/j.bioorg.2013.12.001.

References

[1] K. Hostettmann, A. Marston, Chemistry and Pharmacology of Natural Products: Saponins, Cambridge University Press, 1995. p. 326.
[2] D. Frechet, B. Chrıst, Du. Monegier, B. Sorbier, H. Fischer, M. Vuilhorgne, Phytochemistry 30 (3) (1991) 927.
[3] A. Shafagha, M. Shafaghatlonbar, Nat. Prod. Commun. 6 (2) (2011) 275.
[4] V. Vessela, S. Rumyana, K. Ilina, Y. Maya, N. Stefan, M. Mitka, Redox Rep. 16 (2) (2011) 56.
[5] I. Arslan, A. Celik, M.F. Melzig, Bioorg. Med. Chem. 21 (2013) 1179.
[6] G. Tian, L. Zhou, Y. Zhong, W. Xu, H. Bai, L. Liu, S. Cui, Chin. J. Clin. Oncol. 5 (3) (2008) 206.
[7] I. Demir, M. Bayrakcı, K. Mutlu, A.I. Pekacar, Acta Chim. Slov. 55 (2008) 120.
[8] D.R. Richardson, D.S. Kalinowski, S. Lau, P.J. Jansson, D.B. Lovejoy, Biochim. Biophys. Acta 1790 (2009) 702.
[9] A.I. Matesanz, C. Joie, P. Souza, Dalton Trans. 39 (30) (2010) 7059.
[10] C.R. Kowol, R. Berger, R. Eichinger, A. Roller, M.A. Jakupec, P.P. Schmidt, V.B. Arion, B.K. Keppler, J. Med. Chem. 50 (2007) 1254.
[11] M.X. Li, C.L. Chen, D. Zhang, J.Y. Niu, B.S. Ji, Eur. J. Med. Chem. 45 (2010) 3169.
[12] J. Chen, Y.W. Huang, G. Liu, Z. Afrasiabi, E. Sinn, S. Padhye, Y. Maa, Toxicol. Appl. Pharmacol. 197 (2004) 40.
[13] I.H. Hall, K.G. Rajendran, D.X. West, A.E. Liberta, Anticancer Drugs 4 (2) (1993) 231.
[14] Y. Gok, H. Ertepinar, S.Z. Yildiz, Spectrosc. Lett. 23 (1990) 713.
[15] V.B. Rana, J. Inorg. Nucl. Chem. 1975 (1826) 37;
R.K. Agarwal, S. Parasad, Turk. J. Chem. 29 (2005) 289.
[16] B.D. Sarma, J.C. Bailer Jr., J. Am. Chem. Soc. 77 (1955) 5476.
[17] (a) S. Chandra, K.K. Sharma, Synth. React. Inorg. Metal–Org. Chem. 12 (1982) 415;
(b) S. Chandra, K.B. Pandeya, Transit. Metal Chem. 6 (1981) 110.
[18] (a) A. Bilgin, Y. Gok, Synth. React. Inorg. Metal–Org. Chem. 31 (2001) 1717;
(b) R. Gup, H.K. Alpguz, A.D. Beduk, Collect. Czech. Chem. Commun. 67 (2002) 209;
(c) G. Gümüs, I. Gürol, F. Yuksel, A.G. Gürek, V. Ahsen, Polyhedron 33 (2012) 45;
(d) A. Zülfıkaroğlu, C.Y. Ataol, H. Bati, O. Büyükgüngör, J. Coord. Chem. 65 (9) (2012) 1525.
[19] I. Babahan, E. Poyrazoglu Coban, H. Biyik, Maejo Int. J. Sci. Technol. 7 (01) (2013) 26.
[20] I. Babahan, E. Poyrazoglu Coban, A. Ozmen, H. Biyik, B. Isman, Afr. J. Microbiol. Res. 5 (3) (2011) 271.
[21] R. Güp, Russ. J. Coord. Chem. 32 (2006) 99.
[22] M. Macit, H. Batı, B. Batı, Turk. J. Chem. 24 (2000) 81.
[23] A. Kılıc, E. Tas, B. Gumgum, A. Yilmaz, Chin. J. Chem. 24 (2006) 1599.
[24] E. Canpolat, M. Kaya, J. Coord. Chem. 58 (2005) 1217.
[25] E. Canpolat, Kaya, J. Coord. Chem. 55 (8) (2002) 961.
[26] E. Ozcan, E. Karapınar, B. Demirtas, Transit. Metal Chem. 27 (2002) 557.
[27] A. Bilgin, Y. Gok, Synth. React. Inorg. Metal–Org. Chem. 31 (9) (2001) 1717.
[28] M. Dolaz, M. Tumer, A. Golcu, Turk. J. Chem. 25 (2001) 491.

[29] S. Serin, Transit. Metal Chem. 26 (2001) 300.
[30] E. Tas, M. Ulusoy, M. Guler, Synth. React. Inorg. Metal–Org. Chem. 34 (7) (2004) 1211.
[31] S.Y. Ucan, B. Mercimek, Synth. React. Inorg. Metal–Org. Nano-Metal Chem. 35 (2005) 197.
[32] E. Tas, A. Cukurovali, M. Kaya, J. Coord. Chem. 44 (1998) 109.
[33] D.S. Kumar, K.V. Sharathnath, P. Yogeswaran, A. Harani, K. Sudhakar, P. Sudha, D. Banji, Int. J. Pharmacol. Sci. Rev. Res. 1 (2) (2010). Article 018.
[34] I. Podolak, A. Galanty, D. Sobolewska, Phytochem. Rev. 9 (3) (2010) 425.
[35] N. Garçon, M. Van Mechelen, Expert Rev. Vaccines 10 (4) (2011) 471.
[36] A. Jemal, R. Siegel, E. Ward, T. Murray, J. Xu, M.J. Thun, CA Cancer J. Clin. 57 (2007) 43.
[37] W.R. Brian, Master Thesis, Virginia Polytechnic Institute and State University, 1984.
[38] M. Grusch, D. Polgar, S. Gfatter, K. Leuhuber, S. Huettenbrenner, C. Leisser, G. Fuhrmann, F. Kassie, H. Steinkellner, K. Smid, G.J. Peters, H.N. Jayaram, W. Klepal, T. Szekeres, S. Knasmuller, G. Krupitza, Cell Death Differ. 9 (2) (2002) 169.